Published in final edited form as:
Magn Reson Imaging Clin N Am. 2008 November ; 16(4): 613–viii. doi:10.1016/j.mric.2008.07.008.

BOLD MRI of the Kidneys

Lu-Ping Li, PhD, **Sarah Halter, BA**, and **Pottumarthi V. Prasad, PhD**
Center for Advanced Image, Department of Radiology, Evanston Northwestern Healthcare, Evanston, IL & Northwestern University Medical School, Chicago, IL

Synopsis

Oxygenation status plays a major role in renal physiology and pathophysiology and hence has attracted considerable attention in recent years. While much of the early work and a significant amount of present work is based on invasive methods or *ex vivo* analysis and hence restricted to animal models, BOLD (blood oxygen level dependent) MRI has been shown to extend these findings to humans. BOLD MRI is most useful in monitoring effects of physiological or pharmacological maneuvers. Several teams around the world have demonstrated reproducible data and have illustrated several useful applications. Studies supporting the use of renal BOLD MRI in characterizing disease with prognostic value have also been reported. Here, an overview of the current state-of-the art of renal BOLD MRI is provided.

Keywords

BOLD; kidney; MRI; oxygenation; blood flow; renal failure

Introduction

Renal oxygenation status is receiving greater attention from both the scieintific and clinical communities [1–3]. In most organs, regional oxygen tension (pO_2) closely follows the level of regional blood flow, since oxygen consumption is relatively constant. But this is not true in the kidney, where active tubular reabsorption demands more oxygen consumption whenever filtration and blood flow rise together [4]. Over a wide range of normal blood flows the renal arterio-venous oxygen gradient is remarkably constant. For the purposes of function and oxygen supply, the mammalian kidney can be considered to be made of two separate organs, cortex and medulla [4]. The flow of blood to the renal cortex normally supplies oxygen far in excess of its metabolic needs. By contrast, blood flow to the renal medulla is parsimonious. In addition, oxygen diffuses from the arterial to venous *vasa recta*, and the process of generating an osmotic gradient by active reabsorption of sodium requires large amount of oxygen. All these combined, result in a poorly oxygenated medulla. A non-invasive method to evaluate this heterogeneous distribution of oxygen availability within the kidney is highly desirable. Blood oxygenation level dependent (BOLD) MRI has been shown to be useful in evaluating intra-renal oxygenation status both in animal models and in humans. In this article, we provide

Corresponding author for proof and reprints: Pottumarthi V. Prasad, Radiology Department / Center for Advanced Imaging, Walgreen Building, Suite G507, Evanston Hospital, 2650 Ridge Avenue, Evanston, IL 60201, Tel: (847) 570-1349, E-mail: pprasad@enh.org. Coauthor(s) address(es): Luping Li and Sarah Halter, Radiology Department / Center for Advanced Imaging, Walgreen Building, Suite G507, Evanston Hospital, 2650 Ridge Avenue, Evanston, IL 60201, Tel: (847) 570-1948, E-mail: lli2@enh.org

an overview of the method, and review the current state-of-the-art in terms of technique implementation and applications.

Renal medullary hypoxia and its consequences

Intra-renal oxygenation is an important determinant in renal pathophysiology, both in acute [5–7] and chronic settings [3,8,2]. It is now well established that the renal medulla functions at a significantly low ambient pO_2 (<20 mm of Hg), lower compared to even systemic venous blood (~40 mm of Hg). This is a consequence of lower blood flow to the medulla and the counter current arrangement of blood vessels permitting oxygen diffusion from the arterial to venous *vasa recta*. At the same time, the medullary thick ascending limbs are responsible for the generation of an osmotic gradient by active reabsorption of sodium, a process that requires a large amount of oxygen. A limited oxygen supply and heavy demand results in the renal medulla operating at extremely low levels of pO_2 making it vulnerable to hypoxic injury [1].

Compromised renal perfusion (ischemic ARF) and nephrotoxins are responsible for most episodes of acute renal failure [5]. Inadequate blood flow can be due to renal artery stenosis, occlusion, intrarenal small vessel lesions such atherosclerosis, atheroemboli, or vasculitis [9]. The functional integrity of microvasculature depends on the proper balance between vasoconstrictive and vasodilatory factors. Damage to the endothelium or alteration in endothelial function can result in local vasoconstriction due to increased production of vasoconstrictive substances such as endothelin and/or decreased production of vasodilatory substances such as nitric oxide. Alterations in endothelial cell function can be important in the local loss of autoregulation that occurs in ischemic renal failure [10]. Nephrotoxicity caused by substances like iodinated contrast or nonsteroidal anti-inflammatory drugs is thought to be due to acute alterations in renal blood flow [5]. Renal hypoxia also plays a key role in the initiation and progression of chronic kidney disease (CKD) [3,8,2]. A combination of microvascular changes and differences in oxygen consumption lead to enhanced hypoxia in the chronic setting.

BOLD MRI: a method for non-invasive evaluation of intra-renal oxygenation

Most data on renal hypoxia have been based on invasive microelectrode techniques in rodent models [11–15]. Other methods include histological staining based on pimonidazole [16–18], electron paramagnetic resonance [19,20], or fluorine-19 MRI using a fluorinated blood substitute [21,22]. To date none of these are considered viable for human applications.

BOLD MRI uses the paramagnetic properties of deoxyhemoglobin to acquire images sensitive to local tissue oxygen concentration. As the deoxyhemoglobin concentration in blood increases, the T_2* relaxation time of the protons decreases and more dephasing occurs in the surrounding tissues [23]. This produces measurable signal loss in areas of increased deoxyhemoglobin concentration. BOLD MRI has been used extensively in organs such as the brain [24–27]. Changes in oxygen saturation of Hb associated with changes in blood pO_2 are most marked at low levels of pO_2 [28]. This makes BOLD MRI ideally suited for oxygenation measurements in the renal medulla, where pO_2 is normally in the range of 15 to 20 mm Hg [1,29].

Renal BOLD MRI Acquisition Techniques

Single shot echo planar imaging (EPI) is the technique commonly utilized for functional brain imaging and is readily applicable to the abdomen [30,31]. However, EPI has a high sensitivity to magnetic susceptibility differences resulting in image distortions, signal loss and limited spatial resolution. While spatial resolution and image quality may be compromised, EPI offers high temporal resolution. It may be advantageous for applications where fast changes are expected and when R_2* mapping is not necessary.

A multiple gradient-recalled-echo (mGRE) sequence is currently the most widely used for renal BOLD MRI [32]. The mGRE technique provides R_2* (= $1/T_2$*) maps with improved SNR (signal to noise ratio), spatial resolution and image quality compared to the EPI method. The 2-D mGRE technique acquires multiple gradient echoes (typically 8 to 16) following each excitation pulse, resulting in 8 to 16 images with different echo times to be used to fit for R2*. For optimal SNR, the maximum echo time should be approximately equal to the T_2* value of interest (in this case, the medulla). At 1.5 T, medullary T_2* ~ 50 ms and at 3.0 T it is ~ 25 ms. In other words, maximum TE should be about 50 ms at 1.5T and 25 ms at 3.0T. With TR of 50 to 100 ms, entire acquisition can be obtained within a breath hold interval. A 3-D implementation has been shown to achieve full kidney coverage within a breath-hold time [33,34]. The benefit of a 3-D technique is the increased signal noise ratio when compared to 2-D mGRE with sequential multi-slice acquisition with comparable spatial coverage.

Selective water excitation technique avoids any potential chemical shift artifacts and amplitude modulations due to different phase accumulations between water and fat on GRE images [35]. This technique eliminates fat signals and avoids confusion between renal sinus fat and medulla on the R_2* maps [32]. However, the selective excitation pulses increase scan time [36] and it may not be necessary when ROIs are defined based on the anatomic template [32].

Renal BOLD MRI Data Analysis

In functional brain MRI, T_2* (=$1/R_2$*) weighted signal intensity (SI) is used for analysis. This is primarily due to the fact that the observed differences are small (typically < 5% change in signal intensity during activation). While changes in signal intensity can be translated to changes in R_2* (ΔR_2* = ΔSI /TE), measurement of R_2* is not performed routinely. R_2* changes have been estimated to be on the order of 0.5 s^{-1} at 1.5 T [37]. In the kidneys, ΔR_2* in the medulla are typically 5 to 10 s^{-1} and high temporal resolution is not a necessity. So, calculation of R_2* is desirable to compare two measurements from different time points or different subjects. Signal intensity on the other hand will depend on the scanner settings and potentially could be different even within the same subject scanned at different time points. With EPI, one has to acquire images with different echo times. Since the bulk susceptibility effects scale with echo times, R_2* mapping is usually not attempted and ROI analysis are performed to calculate regional R_2*.

R_2* can be calculated as the slope of the straight line fit to Ln (SI) *vs.* echo time data [30], or by fitting the signal intensity *vs.* TE data to a single decaying exponential function. By calculating R_2* pixel by pixel, an R_2* map can be generated. Regions of interest defined on the anatomical template can be used for estimation of R_2* in the renal medulla and cortex. Areas affected by susceptibility artifacts (e.g. Figure 1) should be excluded. Artifacts due to bulk susceptibility differences appear dark even on the low echo time images and show up very bright on the R_2* maps.

Some investigators prefer to use a color scale to display R_2* maps [38–40]. While they provide some advantages in terms of visualization, there is not any fundamental difference in terms of information content. Use of standardized color bars would be necessary for comparison purposes.

Advantage of higher field strength

The potential advantage of high field strength for MRI is that it increases the SNR and/or spatial resolution [41]. Signal changes due to BOLD effects also scale with magnetic field strength. However, chemical shift, susceptibility, flow, and patient motion artifacts can also increase at higher field strengths [42,43].

Recent studies have demonstrated the advantage of 3.0T for renal BOLD MRI compared to 1.5T [44,33]. The cortico-medullary contrast on the R_2* map is significantly improved at 3.0T, with no evidence of increased level of bulk susceptibility artifacts (Fig. 1). The magnitude of the baseline renal medullary R_2* at 3.0T (37.4±1.2 Hz) is roughly twice as large as that at 1.5T (21.8 ± 1.2 Hz) (see Fig. 2) [44]. Similarly, changes in R2* after pharmacologic maneuver resulted in roughly twice the response at 3.0 T compared to 1.5 T [33,44].

Validation of renal BOLD MRI for evaluation of intra-renal oxygenation

Preliminary validation of the renal BOLD MRI measurements were performed by comparing previously published data in rat kidneys using invasive microelectrodes [11] to observe trends, such as response to furosemide *vs.* acetazolamide [30,32]. Acetazolamide is a diuretic similar to furosemide, but acts on a cortical portion of the nephron, and hence has minimal effect on medullary oxygen consumption. There have also been reports comparing BOLD MRI with simultaneously acquired measurements using invasive electrodes in the contralateral kidneys of swine [45]. By varying the inspired gas ratio (oxygen to nitrogen), they observed a linear relationship between R_2* and pO_2 as measured by the electrodes (r=0.67 and 0.73 in medulla and cortex, respectively). Using this relationship, Simon-Zoula and colleagues [46] converted their R_2* measurements in human kidneys and estimated the pO_2 of 42 mmHg in the medulla and 50 mmHg in cortex. However, it should be noted that such calibration is strictly valid only for the kidneys in which the simultaneous measurements were obtained.

Reproducibility of renal BOLD MRI measurements

One important aspect of validation is reproducibility. Simon-Zoula and colleagues [46] have reported on short term reproducibility of renal R_2* measurements. Three identical measurements on three axial and three coronal slices of right and left kidneys were performed with a 5 minutes break in between. Subjects were moved from the scanner and a subsequent BOLD scan performed with a complete new calibration. The mean R_2* values determined in medulla and cortex showed no significant differences over three repetitions and low intra-subject coefficients of variation (CV) (3 and 4% in medulla and cortex, respectively). Only a minor influence of slice orientation was observed. The authors also point out a 3% difference between left and right kidneys, which is within their reproducibility variation. In renal transplants, the reproducibility over 65 days was found to be similar [47]. Long term reproducibility (81 – 272 days) in renal R_2* measurements were shown to be within ~12% based on a coefficient of variance analysis [48]. These observations support the feasibility of performing sequential studies in the same subject, *e.g.* with a different pharmacological maneuver.

Renal BOLD MRI Applications

Physiological / Pharmacological induced changes in intra-renal oxygenation

BOLD MRI is most effective in monitoring changes induced by pharmacological / physiological maneuvers [30,32,49–53]. The most widely applied maneuver is administration of furosemide [52,44,33]. Figure 3 and Figure 4 are related and should be described in the same part of this review. Figure 3 illustrates the differences in R_2* map pre- and post- administration of furosemide. Figure 4 [33] shows the temporal response in R_2* both in cortex and medulla following administration of furosemide in a representative subject. This clearly points to the sensitivity of the technique to follow changes in renal oxygenation. Water load is another simple and effective maneuver to acutely change medullary oxygenation [53,49,34]. The observed improvement in medullary oxygenation (lower R_2*) has been shown to be related to endogenous prostaglandin production [49,34]. This maneuver has also been shown to differentiate responses in elderly (Fig. 5) [49] and diabetics [53] compared to healthy young subjects.

Vasoactive substances influence intrarenal oxygenation and hence could be monitored using BOLD MRI. Chronic infusions of angiotensin II have been shown to diminish renal perfusion [54] and are expected therefore to reduce renal oxygenation. This was recently confirmed by the BOLD MRI measurement in healthy subjects where angiotensin II caused a shortening of BOLD T_2* in renal cortex [31]. Sodium nitroprusside and norepinephrine, although of equal potency concerning blood pressure responses, did not alter the renal BOLD signal, probably due to autoregulation. Angiotensin II is known to override the autoregulation.

Nitric oxide (NO) is a soluble gas that is continuously synthesized by the endothelium [55] and has a wide range of biological properties including relaxation of vascular tone. In rat kidneys, administration of L-NAME (a nitric oxide synthase inhibitor) resulted in further increase in medullary R_2* suggesting enhanced hypoxia [56]. Interestingly, such an increase was absent in a genetic model of hypertension [56] and was shown to be restored when treated with an anti-oxidant [57]. Preliminary data in a small number of healthy young human subjects with NOSi have been reported [58].

Several pharmaceuticals are known to adversely influence renal hemodynamics and, subsequently, affect renal oxygenation. Since renal hypoxia is implicated in the development of drug-induced renal failure, monitoring the effects of these drugs would help for a better understanding of the pathophysiology and hence help in developing appropriate methods to clinically manage acute renal failure. Contrast medium-induced nephropathy (CIN) is a well-known cause of acute renal failure, but the development of CIN remains poorly understood [59]. Iodinated contrast medium iopromidum produced an increase in medullary and cortical R_2* values in humans 20 min after administration [60].

Calcineurin inhibitors, cyclosporine micro-emulsion (CsA-ME) and tacrolimus are currently the most widely used baseline immunosuppressants for prevention of acute rejection following kidney transplantation. However, their use is associated with acute and chronic toxicity. A significant reduction in medullary R_2* values (suggesting improvement in oxygenation) was observed 2 h after CsA-ME administration in healthy subjects [60]. This is in apparent contradiction to the previously reported decrease in renal blood flow related to afferent arteriolar vasoconstriction [61]. However, the study also suggested reduced in GFR and it is possible that there is an associated reduction in oxygen consumption related to reduced sodium reabsorption in the medulla. Tacrolimus had no significant effect on R_2* values for medulla or cortex in healthy subjects [60], even though the nephrotoxic effects are known to be similar to CsA. Further studies are necessary to fully evaluate the significance of these observations.

Non-steroidal anti-inflammatory drugs (NSAID) are the most commonly used medicines to reduce ongoing inflammation, pain, and fever [62]. Chronic use is known to be associated with gastrointestinal, renal and even cardiac effects [63,64]. NSAIDs block the synthesis of vasodilatory prostaglandins and hence reduce renal perfusion [1]. Indomethacin has been shown to reduce medullary oxygenation by microelectrodes [65] and BOLD MRI [50] in rat kidneys. However, it did not induce a significant change in renal medullary R_2* in healthy subjects [60]. This might indicate that a single dose of indomethacin as prescribed routinely does not significantly influence renal oxygenation in humans. Similarly, another common NSAID, ibuprofen did not change baseline renal medullary and cortical R_2* [52]. However, administration of ibuprofen (and similarly naproxen) significantly reduced the response to water load [49,34]. This may suggest that use of a provocative maneuver such as water load may be necessary to evaluate effects of prostaglandin inhibition.

Renal BOLD MRI in disease

Renal artery stenosis (RAS)—is a common cause of ischemia and hence has consequences to intra-renal oxygenation. Juillard and colleagures [66] used a well designed pre-clinical

model to test if BOLD can detect the presence of renal hypoxia induced by RAS. They found that R_2* relaxivity increased continuously and progressively in parallel with the decrease in RBF (renal blood flow) in response to increasing levels of stenosis, suggesting evolving hypoxia in both the medulla and cortex. The authors offered the following concluding remarks, 'new functional tools, such as BOLD, capable of detecting ischemia and characterizing patterns of intra-renal oxygen levels, may assist in identifying patients that would be more likely to benefit from therapeutic procedures.' Alford et al [67] also documented an increase in R_2* following acute occlusion of renal artery. Contralateral kidney showed no such change. They also demonstrated that the R_2* returned to baseline values upon releasing the occlusion. Recently, Textor *et al* [68] reported on measurements in human subjects with RAS. In normal-sized kidneys downstream of high-grade renal arterial stenoses, R_2* was elevated at baseline (suggesting enhanced hypoxia) and fell after administration of furosemide. This was true even when the GFR was significantly reduced. These results are supported by previous reports of preserved cortical tissue volume in poststenotic kidneys, despite reduced function as measured by isotope renography [69]. These in turn may suggest that GFR might be recoverable for such cases and that nonfiltering kidney tissue represents a form of "hibernation" in the kidney with the potential for restoring kidney function after restoring blood flow [69]. On the other hand, atrophic kidneys beyond totally occluded renal arteries demonstrated low levels of R_2* (improved oxygenation) that did not change after furosemide [68]. This may suggest non-functioning kidney with limited or no oxygen consumption. The article also includes an example where a kidney with multiple arteries showed different R_2* values in regions supplied by a stenosed renal artery. Given the recent concerns with nephrogenic systemic fibrosis (NSF) [70–73]—use of contrast enhanced MRA and evaluation of GFR in subjects with compromised renal function need additional caution. Non-contrast methods, such as BOLD MRI, may provide important alternative techniques for investigating vascular compromise and renal functional status.

Unilateral ureteral obstruction—Pedersen *et al* [45] demonstrated changes on BOLD MRI in a pig model of unilateral ureteral obstruction (UUO). Twenty-four hours of UUO was associated with an increased R_2* in the cortex and a decreased R_2* in medulla as compared with the baseline indicating that pO_2 levels were reduced in the cortex and increased in the medulla during and after release of obstruction. Similar result was observed by Thoeny et al in 10 patients with a distal unilateral urethral calculus [74]. All patients had significantly lower medullary and cortical R_2* values in the obstructed kidney than in the nonobstructed kidney. The increase in oxygen content in medulla may due to a decrease in oxygen consumption as a result of reduced GFR in obstructed kidney. R_2* in the obstructed kidneys were also significantly lower than the kidneys of healthy subjects.

Diabetes mellitus—Renal involvement in diabetes mellitus is the main cause of end-stage renal failure and a leading cause of morbidity and mortality in diabetic patients [75]. Renal hypoxia has long been a suspect in the development of renal failure from diabetes mellitus. A recent animal study using invasive microelectrodes has shown that the pO_2 in chronic diabetic rats is decreased throughout the renal parenchyma [76]. Ries and colleagues observed in an animal model that the diabetic kidney showed significantly lower oxygenation level in renal medulla compared to a control group using BOLD MRI at 5 days post induction [77]. A similar study [78] with BOLD MRI along with invasive blood flow and oxygenation measurement by optical fiber probes showed that the pO_2 was considerably lower in diabetic rats after 2-, 5-, 14-, and 28 days following induction of diabetes compared to control rats. No blood flow changes were observed in both diabetes and normal groups over this time period, suggesting that the reduced oxygenation was related to increased consumption probably related to hyperfiltration. Furthermore, there was a significant and progressive decrease in the renal oxygenation by fiber-optic probe in diabetic animals compared to control group over time. The

increase in the BOLD signal was also progressive with the highest increase observed with the 28-day group for both renal medulla and cortex.

BOLD MRI has also been used to evaluate diabetic human subjects. A study of eighteen human subjects (nine healthy non-diabetics and nine with mild, controlled diabetes) [53] showed that in the healthy, water-diuresis led to a significant increase in the oxygenation of the renal medulla, but not in the diabetic patients as evaluated by BOLD MRI. These results suggest that even patients with mild diabetes already show signs of renal injury long before the onset of symptoms that usually accompany kidney disease, and a likely deficiency in the synthesis of endogenous vasodilator substances, like prostaglandin or NO.

BOLD MRI may provide important insight into the pathophysiology of renal injury at early stages in diabetes and allow for means to evaluate novel drug interventions especially those targeting renal hypoxia.

Hypertension—The kidney is believed to play a role in the pathogenesis of essential hypertension [79,80]. In particular, reduced renal medullary blood flow is thought to be one of the important factors in the development of the disease [81]. Animal studies have shown that medullary blood flow is decreased in hypertension and, more importantly, that reduced medullary blood flow is sufficient to produce hypertension [82].

A study using BOLD MRI technique showed that medullary R_2* increased significantly in control rats in response to NOS inhibition while hypertensive rats exhibited a minimal change [56]. The baseline R_2* in hypertensive rats were found to be comparable to post-L-NAME values in controls, suggesting a basal deficiency of nitric oxide in hypertension rats [56]. This observation was consistent with previous reports based on invasive blood flow measurement [83–89].

Tempol (4-hydroxy-2,2,6,6-tetramethyl piperidinoyl) is a superoxide scavenger and is known to improve NO bioavailability. Short- and long-term administration of tempol has been shown to increase medullary blood flow in hypertension rats by 35–50% and reduce mean arterial pressure (MAP) by 20 mmHg compared with untreated hypertension rats as evaluated by invasive technique [90–93]. Tempol showed no effect on the R_2* in normal rats but significantly decreased in hypertensive rats evaluated by BOLD MRI [57]. The degree of R_2* changes is in qualitative agreement with the observed medullary blood flow and MAP changes induced by tempol administration assessed by invasive measurement [90].

These studies combined with the report on Angiotensin II [31] support a role for BOLD MRI in the understanding of pathophysiology of hypertension and potentially play a role in the evaluation of novel drug interventions.

Renal Allografts—Kidney transplantation allows patients with end-stage renal disease to leave close to normal lives. However, graft dysfunction is a major concern and early characterization of the underlying cause of graft dysfunction is important. Delayed treatment can lead to the irreversible loss of nephrons and hasten graft loss over time [94,95]. Allograft rejection and acute tubular necrosis (ATN) are two important causes of early kidney allograft dysfunction, and it is difficult to discriminate between them by regular clinical tests. Percutaneous transplant biopsy is the most effective method, but it has risks such as bleeding, kidney rupture, and rarely, graft loss [96,97]. Developing a non-invasive method may be highly desirable. Several groups have evaluated the feasibility of BOLD MR imaging in patients with renal allografts.

Thoeny and colleagues [47] compared the BOLD index between transplanted kidney and the native kidney in healthy volunteers. The medullary R_2* was found to be lower in transplant patients than in healthy volunteers ($P < .004$) implying a relatively improved oxygenation in transplanted kidney. This could be explained as the result of reduced tubular fractional reabsorption of sodium and increased blood flow due to allograft denervation. We believe that these observations may also be influenced by the time of the study following transplantation.

Sadowski and colleagues [98] evaluated 20 patients who had recently received renal transplants in an attempt to obtain preliminary data on potential differences between normal functioning transplants and those experiencing acute rejection and acute tubular necrosis (ATN). Six patients had clinically normal functioning transplants, eight had biopsy-proved rejection, and six had biopsy-proven ATN. Their results showed that R_2* measurements in the medullary regions of transplanted kidneys with acute rejection were significantly lower than those in normally functioning transplants or transplants with ATN. It is also suggested that using a threshold R_2* value of 18 s^{-1}, acute rejection could be differentiated from normal function and ATN in all cases. The authors comment, “this is important because if MR imaging can help exclude acute rejection, a substantial number of percutaneous transplant biopsies could be avoided. Furthermore, clinicians weigh their concern that acute rejection is actually present against the risks of percutaneous biopsy. Patients are often watched over a period of time so that trends in laboratory values can be evaluated before a decision is made to proceed with biopsy. Having a noninvasive means of determining the presence of acute rejection could allow patients to be evaluated without the concerns associated with percutaneous biopsy. This, in turn, would lead to an increase in the screening of patients and, potentially, earlier detection of kidney transplant rejection.” Similar findings were reported by a more recent study in a much larger number of subjects (n = 82) including biopsy-proven acute rejection and ATN (Fig. 6) [40].

Djamali and colleagues applied BOLD-MRI to discriminate different types of rejection early after kidney transplantation [99]. Twenty-three patients underwent imaging in the first four months post-transplant. Five had normal functioning transplants and 18 had biopsy-proven acute allograft dysfunction, acute tubular necrosis and acute rejection including borderline rejection: n=3; IA rejection: n=4; IIA rejection: n=6: C4d(+) rejection: n=9. Their results in general agreed with those of Sadowski *et al* [98] in that medullary R_2* levels were higher (increased local deoxyhemoglobin concentration) in normal functioning allografts (24.3/s±2.3) compared to acute rejection (16./s±2.1) and ATN (20.9/s±1.8) ($p<0.05$). There was no statistically significant difference in cortical R_2*. Medullary R_2* was the lowest in acute rejection with a vascular component, *i.e.* IIA and C4d (+) compared to IA and “borderline” rejection. Receiver operator characteristic (ROC) curve analyses suggested that medullary R_2* and medullary-cortical ratio could accurately discriminate acute rejection in the early post-transplant period.

Chronic allograft nephropathy (CAN) is the leading cause of kidney transplant failure [100]. A better understanding of CAN's pathogenesis may lead to the development of strategies to prevent or delay its development or progression. Djamali *et al* [38] used BOLD MRI to evaluate patients with CAN and looked for correlations with other conventional biomarkers of oxidative stress. Similar to previous reports on acute rejection, subjects with CAN showed lower medullary and cortical R_2* values. More importantly, they observed that intra-renal oxygenation as evaluated by BOLD MRI showed a high level of correlation with serum and urine biomarkers of oxidative stress. They concluded, “this pilot study is provocative in suggesting that oxygenation patterns are different in CAN and, moreover, are strongly associated with oxidative stress. Our therapeutics to date have not used oxygen delivery as an outcome of therapy, but it may well be the case that optimal tissue oxygenation, not hypoxia nor hyperoxia, is a target of therapy. The association in CAN between aberrant kidney

oxygenation and oxidative stress is important and may provide leads as to how to slow loss of transplant function."

Renal BOLD MRI: limitations

Several limitations of BOLD MRI technique have to be considered. BOLD signal depends more on field inhomogeneity contributions and can be influenced by oxygen supply, oxygen consumption, blood flow [101,25], blood volume [101,25], hematocrit [102], and pO_2 [103]. Moreover, changes in the oxygen-hemoglobin dissociation curve may be influenced by factors such as pH and temperature [104]. In addition, R_2* is influenced by the vessel geometry and applied pulse sequence parameters. Therefore, the absolute magnitude of R_2* are less reliable in practice than the relative changes observed. For the same reason, a direct calibration of R_2* vs. pO_2 has to be viewed with caution.

Susceptibility artifacts caused by bowel gas [105] are sometimes marked, and at times lead to noninterpretable observations. Motion artifacts due to breathing should also be carefully monitored. Use of respiratory monitor could minimize errors due to improper breath-holding.

Because hydration status can significantly influence the renal BOLD MRI measurements, it is preferred to perform studies following 12 hour fasting (overnight). This would facilitate combining data from different individual subjects and comparison of different groups of subjects.

Summary

BOLD MRI is an endogenous contrast mechanism and allows for rapid, noninvasive means to assess intra-renal oxygenation both in animal models and humans. To-date the method has been shown to be reproducible within and across several laboratories throughout the world. The technique is most efficacious in evaluating physiological or pharmacological maneuvers that can influence renal oxygenation status. This may have important applications in understanding renal physiology and pathophysiology, and in turn lead to the development of novel interventional strategies. The technique has been shown to be of value in characterizing disease that can potentially influence patient management, *e.g.* identifying kidneys that may be amenable to functional recovery by restoring blood flow in cases with renal artery stenosis and distinguishing between acute rejection from acute tubular necrosis in renal transplants. In a recent editorial, Drs. Wang and Yeh [106] comment "the assessment of renal oxygenation could potentially provide insights into early derangements of renal physiology and function prior to the onset of irreversible renal injury". They further conclude, "BOLD MRI imaging promises to become an important tool for monitoring renal oxygenation in various clinical scenarios".

Acknowledgements

This work supported in part by a grant from the National Institutes of Health, DK-53221 (PVP).

References

1. Brezis M, Rosen S. Hypoxia of the renal medulla--its implications for disease. N Engl J Med 1995;332 (10):647–655. [PubMed: 7845430]
2. Norman JT, Fine LG. Intrarenal oxygenation in chronic renal failure. Clin Exp Pharmacol Physiol 2006;33(10):989–996. [PubMed: 17002678]
3. Eckardt KU, Bernhardt WM, Weidemann A, et al. Role of hypoxia in the pathogenesis of renal disease. Kidney Int Suppl 2005;99:S46–S51. [PubMed: 16336576]

4. Epstein FH, Agmon Y, Brezis M. Physiology of renal hypoxia. Ann N Y Acad Sci 1994;718:72–81. [PubMed: 8185253]discussion 81-72
5. Thadhani R, Pascual M, Bonventre JV. Acute renal failure. N Engl J Med 1996;334(22):1448–1460. [PubMed: 8618585]
6. Rosenberger C, Rosen S, Heyman SN. Renal parenchymal oxygenation and hypoxia adaptation in acute kidney injury. Clin Exp Pharmacol Physiol 2006;33(10):980–988. [PubMed: 17002677]
7. Heyman SN, Fuchs S, Brezis M. The role of medullary ischemia in acute renal failure. New Horiz 1995;3(4):597–607. [PubMed: 8574590]
8. Nangaku M. Chronic hypoxia and tubulointerstitial injury: a final common pathway to end-stage renal failure. J Am Soc Nephrol 2006;17(1):17–25. [PubMed: 16291837]
9. Bonventre JV. Mechanisms of ischemic acute renal failure. Kidney Int 1993;43(5):1160–1178. [PubMed: 8510397]
10. Conger JD, Robinette JB, Schrier RW. Smooth muscle calcium and endothelium-derived relaxing factor in the abnormal vascular responses of acute renal failure. J Clin Invest 1988;82(2):532–537. [PubMed: 3261301]
11. Brezis M, Agmon Y, Epstein FH. Determinants of intrarenal oxygenation. I. Effects of diuretics. Am J Physiol 1994;267(6 Pt 2):F1059–F1062. [PubMed: 7810692]
12. Brezis M, Heyman SN, Epstein FH. Determinants of intrarenal oxygenation. II. Hemodynamic effects. Am J Physiol 1994;267(6 Pt 2):F1063–F1068. [PubMed: 7810693]
13. Dinour D, Brezis M. Effects of adenosine on intrarenal oxygenation. Am J Physiol 1991;261(5 Pt 2):F787–F791. [PubMed: 1951710]
14. Brezis M, Heyman SN, Dinour D, et al. Role of nitric oxide in renal medullary oxygenation. Studies in isolated and intact rat kidneys. J Clin Invest 1991;88(2):390–395. [PubMed: 1864953]
15. Heyman SN, Rosen S, Fuchs S, et al. Myoglobinuric acute renal failure in the rat: a role for medullary hypoperfusion, hypoxia, and tubular obstruction. J Am Soc Nephrol 1996;7(7):1066–1074. [PubMed: 8829123]
16. Rosenberger C, Goldfarb M, Shina A, et al. Evidence for sustained renal hypoxia and transient hypoxia adaptation in experimental rhabdomyolysis-induced acute kidney injury. Nephrol Dial Transplant 2008;23(4):1135–1143. [PubMed: 18048419]
17. Rosenberger C, Khamaisi M, Abassi Z, et al. Adaptation to hypoxia in the diabetic rat kidney. Kidney Int 2008;73(1):34–42. [PubMed: 17914354]
18. Tanaka T, Kato H, Kojima I, et al. Hypoxia and expression of hypoxia-inducible factor in the aging kidney. J Gerontol A Biol Sci Med Sci 2006;61(8):795–805. [PubMed: 16912095]
19. Swartz HM, Clarkson RB. The measurement of oxygen in vivo using EPR techniques. Phys Med Biol 1998;43(7):1957–1975. [PubMed: 9703059]
20. Gallez B, Jordan BF, Baudelet C, et al. Pharmacological modifications of the partial pressure of oxygen in murine tumors: evaluation using in vivo EPR oximetry. Magn Reson Med 1999;42(4): 627–630. [PubMed: 10502749]
21. Hunjan S, Zhao D, Constantinescu A, et al. Tumor oximetry: demonstration of an enhanced dynamic mapping procedure using fluorine-19 echo planar magnetic resonance imaging in the Dunning prostate R3327-AT1 rat tumor. Int J Radiat Oncol Biol Phys 2001;49(4):1097–1108. [PubMed: 11240252]
22. Xia M, Kodibagkar V, Liu H, et al. Tumour oxygen dynamics measured simultaneously by near-infrared spectroscopy and 19F magnetic resonance imaging in rats. Phys Med Biol 2006;51(1):45–60. [PubMed: 16357430]
23. Thulborn KR, Waterton JC, Matthews PM, et al. Oxygenation dependence of the transverse relaxation time of water protons in whole blood at high field. Biochim Biophys Acta 1982;714(2):265–270. [PubMed: 6275909]
24. Blatow M, Nennig E, Durst A, et al. MRI reflects functional connectivity of human somatosensory cortex. Neuroimage 2007;37(3):927–936. [PubMed: 17629500]
25. Shen Q, Ren H, Duong TQ. CBF, BOLD, CBV, and CMRO(2) fMRI signal temporal dynamics at 500-msec resolution. J Magn Reson Imaging 2008;27(3):599–606. [PubMed: 18219630]

26. Fukunaga M, Horovitz SG, de Zwart JA, et al. Metabolic origin of BOLD signal fluctuations in the absence of stimuli. J Cereb Blood Flow Metab. 2008
27. Herrmann CS, Debener S. Simultaneous recording of EEG and BOLD responses: a historical perspective. Int J Psychophysiol 2008;67(3):161–168. [PubMed: 17719112]
28. Cherniack MGA, NS.; Kelsen, SG. Physiology. St Louis: C.V. Mosby Company; 1988. Gas exchange and gas transport.
29. Brezis M, Rosen S, Silva P, et al. Renal ischemia: a new perspective. Kidney Int 1984;26(4):375–383. [PubMed: 6396435]
30. Prasad PV, Edelman RR, Epstein FH. Noninvasive evaluation of intrarenal oxygenation with BOLD MRI. Circulation 1996;94(12):3271–3275. [PubMed: 8989140]
31. Schachinger H, Klarhofer M, Linder L, et al. Angiotensin II decreases the renal MRI blood oxygenation level-dependent signal. Hypertension 2006;47(6):1062–1066. [PubMed: 16618841]
32. Prasad PV, Chen Q, Goldfarb JW, et al. Breath-hold R2* mapping with a multiple gradient-recalled echo sequence: application to the evaluation of intrarenal oxygenation. J Magn Reson Imaging 1997;7(6):1163–1165. [PubMed: 9400864]
33. Tumkur S, Vu A, Li L, et al. Evaluation of intrarenal oxygenation at 3.0 T using 3-dimensional multiple gradient-recalled echo sequence. Invest Radiol 2006;41(2):181–184. [PubMed: 16428990]
34. Tumkur SM, Vu AT, Li LP, et al. Evaluation of intra-renal oxygenation during water diuresis: a time-resolved study using BOLD MRI. Kidney Int 2006;70(1):139–143. [PubMed: 16572109]
35. Wehrli FW, Perkins TG, Shimakawa A, et al. Chemical shift-induced amplitude modulations in images obtained with gradient refocusing. Magn Reson Imaging 1987;5(2):157–158. [PubMed: 3586882]
36. Thomasson, DMMJ.; Purdy, DE.; Finn, JP. Optimized water excitation using a phase modulated 1-2-1 binomial pulse train. ISMRM annunal meeting:1994; ismrm; San Francisco, USA. 1994. p. 797
37. Bandettini PA, Wong EC, Jesmanowicz A, et al. Spin-echo and gradient-echo EPI of human brain activation using BOLD contrast: a comparative study at 1.5 T. NMR Biomed 1994;7(1–2):12–20. [PubMed: 8068520]
38. Djamali A, Sadowski EA, Muehrer RJ, et al. BOLD-MRI assessment of intrarenal oxygenation and oxidative stress in patients with chronic kidney allograft dysfunction. Am J Physiol Renal Physiol 2007;292(2):F513–F522. [PubMed: 17062846]
39. Zuo CS, Rofsky NM, Mahallati H, et al. Visualization and quantification of renal R2* changes during water diuresis. J Magn Reson Imaging 2003;17(6):676–682. [PubMed: 12766897]
40. Han F, Xiao W, Xu Y, et al. The significance of BOLD MRI in differentiation between renal transplant rejection and acute tubular necrosis. Nephrol Dial Transplant. 2008
41. Edelstein WA, Glover GH, Hardy CJ, et al. The intrinsic signal-to-noise ratio in NMR imaging. Magn Reson Med 1986;3(4):604–618. [PubMed: 3747821]
42. Yang Y, Gu H, Zhan W, et al. Simultaneous perfusion and BOLD imaging using reverse spiral scanning at 3T: characterization of functional contrast and susceptibility artifacts. Magn Reson Med 2002;48(2):278–289. [PubMed: 12210936]
43. Gonen O, Gruber S, Li BS, et al. Multivoxel 3D proton spectroscopy in the brain at 1.5 versus 3.0 T: signal-to-noise ratio and resolution comparison. AJNR Am J Neuroradiol 2001;22(9):1727–1731. [PubMed: 11673168]
44. Li LP, Vu AT, Li BS, et al. Evaluation of intrarenal oxygenation by BOLD MRI at 3.0 T. J Magn Reson Imaging 2004;20(5):901–904. [PubMed: 15503343]
45. Pedersen M, Dissing TH, Morkenborg J, et al. Validation of quantitative BOLD MRI measurements in kidney: application to unilateral ureteral obstruction. Kidney Int 2005;67(6):2305–2312. [PubMed: 15882272]
46. Simon-Zoula SC, Hofmann L, Giger A, et al. Non-invasive monitoring of renal oxygenation using BOLD-MRI: a reproducibility study. NMR Biomed 2006;19(1):84–89. [PubMed: 16411163]
47. Thoeny HC, Zumstein D, Simon-Zoula S, et al. Functional evaluation of transplanted kidneys with diffusion-weighted and BOLD MR imaging: initial experience. Radiology 2006;241(3):812–821. [PubMed: 17114628]

48. Li LP, Storey P, Pierchala L, et al. Evaluation of the reproducibility of intrarenal R2* and DeltaR2* measurements following administration of furosemide and during waterload. J Magn Reson Imaging 2004;19(5):610–616. [PubMed: 15112311]
49. Prasad PV, Epstein FH. Changes in renal medullary pO2 during water diuresis as evaluated by blood oxygenation level-dependent magnetic resonance imaging: effects of aging and cyclooxygenase inhibition. Kidney Int 1999;55(1):294–298. [PubMed: 9893139]
50. Prasad PV, Priatna A, Spokes K, et al. Changes in intrarenal oxygenation as evaluated by BOLD MRI in a rat kidney model for radiocontrast nephropathy. J Magn Reson Imaging 2001;13(5):744–747. [PubMed: 11329196]
51. Priatna A, Epstein FH, Spokes K, et al. Evaluation of changes in intrarenal oxygenation in rats using multiple gradient-recalled echo (mGRE) sequence. J Magn Reson Imaging 1999;9(6):842–846. [PubMed: 10373033]
52. Epstein FH, Prasad P. Effects of furosemide on medullary oxygenation in younger and older subjects. Kidney Int 2000;57(5):2080–2083. [PubMed: 10792627]
53. Epstein FH, Veves A, Prasad PV. Effect of diabetes on renal medullary oxygenation during water diuresis. Diabetes Care 2002;25(3):575–578. [PubMed: 11874950]
54. Hall JE, Granger JP. Renal hemodynamic actions of angiotensin II: interaction with tubuloglomerular feedback. Am J Physiol 1983;245(2):R166–R173. [PubMed: 6881375]
55. Palmer RM, Ashton DS, Moncada S. Vascular endothelial cells synthesize nitric oxid from L-arginine. Nature 1988;333(6174):664–666. [PubMed: 3131684]
56. Li L, Storey P, Kim D, et al. Kidneys in hypertensive rats show reduced response to nitric oxide synthase inhibition as evaluated by BOLD MRI. J Magn Reson Imaging 2003;17(6):671–675. [PubMed: 12766896]
57. Li LP, Li BS, Storey P, et al. Effect of free radical scavenger (tempol) on intrarenal oxygenation in hypertensive rats as evaluated by BOLD MRI. J Magn Reson Imaging 2005;21(3):245–248. [PubMed: 15723382]
58. Lu-Ping Li, ED.; Pierchala, Linda; Prasad, Pottumarthi. Effect of nitric oxide inhibitor on intrarenal R2* measurements in humans. ISMRM 12th Scientific Meeting and Exhibition: 2004; ISMRM organization; Kyoto, Japan. 2004. p. 565
59. Persson PB, Hansell P, Liss P. Pathophysiology of contrast medium-induced nephropathy. Kidney Int 2005;68(1):14–22. [PubMed: 15954892]
60. Hofmann L, Simon-Zoula S, Nowak A, et al. BOLD-MRI for the assessment of renal oxygenation in humans: acute effect of nephrotoxic xenobiotics. Kidney Int 2006;70(1):144–150. [PubMed: 16641929]
61. Klein IH, Abrahams A, van Ede T, et al. Different effects of tacrolimus and cyclosporine on renal hemodynamics and blood pressure in healthy subjects. Transplantation 2002;73(5):732–736. [PubMed: 11907418]
62. Watson WA, Litovitz TL, Rodgers GC Jr, et al. 2004 Annual report of the American Association of Poison Control Centers Toxic Exposure Surveillance System. Am J Emerg Med 2005;23(5):589–666. [PubMed: 16140178]
63. Fagerholm U, Bjornsson MA. Clinical pharmacokinetics of the cyclooxygenase inhibiting nitric oxide donator (CINOD) AZD3582. J Pharm Pharmacol 2005;57(12):1539–1554. [PubMed: 16354398]
64. Schnitzer TJ, Kivitz AJ, Lipetz RS, et al. Comparison of the COX-inhibiting nitric oxide donator AZD3582 and rofecoxib in treating the signs and symptoms of Osteoarthritis of the knee. Arthritis Rheum 2005;53(6):827–837. [PubMed: 16342089]
65. Heyman SN, Kaminski N, Brezis M. Dopamine increases renal medullary blood flow without improving regional hypoxia. Exp Nephrol 1995;3(6):331–337. [PubMed: 8528677]
66. Juillard L, Lerman LO, Kruger DG, et al. Blood oxygen level-dependent measurement of acute intra-renal ischemia. Kidney Int 2004;65(3):944–950. [PubMed: 14871414]
67. Alford SK, Sadowski EA, Unal O, et al. Detection of acute renal ischemia in swine using blood oxygen level-dependent magnetic resonance imaging. J Magn Reson Imaging 2005;22(3):347–353. [PubMed: 16104014]
68. Textor SC, Glockner JF, Lerman LO, et al. The Use of Magnetic Resonance to Evaluate Tissue Oxygenation in Renal Artery Stenosis. J Am Soc Nephrol. 2008

69. Cheung CM, Shurrab AE, Buckley DL, et al. MR-derived renal morphology and renal function in patients with atherosclerotic renovascular disease. Kidney Int 2006;69(4):715–722. [PubMed: 16395249]
70. Kurtkoti J, Snow T, Hiremagalur B. Gadolinium and nephrogenic systemic fibrosis: association or causation. Nephrology (Carlton) 2008;13(3):235–241. [PubMed: 18221255]
71. Martin DR. Nephrogenic system fibrosis: A radiologist's practical perspective. Eur J Radiol. 2008
72. Penfield JG, Reilly RF Jr. What nephrologists need to know about gadolinium. Nat Clin Pract Nephrol 2007;3(12):654–668. [PubMed: 18033225]
73. Todd DJ, Kagan A, Chibnik LB, et al. Cutaneous changes of nephrogenic systemic fibrosis: predictor of early mortality and association with gadolinium exposure. Arthritis Rheum 2007;56(10):3433–3441. [PubMed: 17907148]
74. Thoeny HC, Kessler TM, Simon-Zoula S, et al. Renal oxygenation changes during acute unilateral ureteral obstruction: assessment with blood oxygen level-dependent mr imaging--initial experience. Radiology 2008;247(3):754–761. [PubMed: 18403623]
75. Knowles HC Jr. Magnitude of the renal failure problem in diabetic patients. Kidney Int Suppl 1974;(1):2–7. [PubMed: 4619133]
76. Palm F, Cederberg J, Hansell P, et al. Reactive oxygen species cause diabetes-induced decrease in renal oxygen tension. Diabetologia 2003;46(8):1153–1160. [PubMed: 12879251]
77. Ries M, Basseau F, Tyndal B, et al. Renal diffusion and BOLD MRI in experimental diabetic nephropathy. Blood oxygen level-dependent. J Magn Reson Imaging 2003;17(1):104–113. [PubMed: 12500279]
78. dos Santos EA, Li LP, Ji L, et al. Early changes with diabetes in renal medullary hemodynamics as evaluated by fiberoptic probes and BOLD magnetic resonance imaging. Invest Radiol 2007;42(3):157–162. [PubMed: 17287645]
79. Cowley AW, Roman RJ, Fenoy FJ, et al. Effect of renal medullary circulation on arterial pressure. J Hypertens Suppl 1992;10(7):S187–S193. [PubMed: 1291653]
80. Johnson RJ, Herrera-Acosta J, Schreiner GF, et al. Subtle acquired renal injury as a mechanism of salt-sensitive hypertension. N Engl J Med 2002;346(12):913–923. [PubMed: 11907292]
81. Cowley AW Jr, Mattson DL, Lu S, et al. The renal medulla and hypertension. Hypertension 1995;25(4 Pt 2):663–673. [PubMed: 7721413]
82. Mattson DL, Roman RJ, Cowley AW Jr. Role of nitric oxide in renal papillary blood flow and sodium excretion. Hypertension 1992;19(6 Pt 2):766–769. [PubMed: 1592478]
83. Dananberg J, Sider RS, Grekin RJ. Sustained hypertension induced by orally administered nitro-L-arginine. Hypertension 1993;21(3):359–363. [PubMed: 8478045]
84. Manning RD Jr, Hu L, Mizelle HL, et al. Cardiovascular responses to long-term blockade of nitric oxide synthesis. Hypertension 1993;22(1):40–48. [PubMed: 7686533]
85. Majid DS, Williams A, Navar LG. Inhibition of nitric oxide synthesis attenuates pressure-induced natriuretic responses in anesthetized dogs. Am J Physiol 1993;264(1 Pt 2):F79–F87. [PubMed: 8430833]
86. Salazar FJ, Alberola A, Pinilla JM, et al. Salt-induced increase in arterial pressure during nitric oxide synthesis inhibition. Hypertension 1993;22(1):49–55. [PubMed: 8319991]
87. Nakanishi K, Mattson DL, Cowley AW Jr. Role of renal medullary blood flow in the development of L-NAME hypertension in rats. Am J Physiol 1995;268(2 Pt 2):R317–R323. [PubMed: 7864223]
88. Mattson DL, Lu S, Nakanishi K, et al. Effect of chronic renal medullary nitric oxide inhibition on blood pressure. Am J Physiol 1994;266(5 Pt 2):H1918–H1926. [PubMed: 8203591]
89. Panza JA, Casino PR, Kilcoyne CM, et al. Role of endothelium-derived nitric oxide in the abnormal endothelium-dependent vascular relaxation of patients with essential hypertension. Circulation 1993;87(5):1468–1474. [PubMed: 8491001]
90. Schnackenberg CG, Welch WJ, Wilcox CS. Normalization of blood pressure and renal vascular resistance in SHR with a membrane-permeable superoxide dismutase mimetic: role of nitric oxide. Hypertension 1998;32(1):59–64. [PubMed: 9674638]

91. Schnackenberg CG, Wilcox CS. Two-week administration of tempol attenuates both hypertension and renal excretion of 8-Iso prostaglandin f2alpha. Hypertension 1999;33(1 Pt 2):424–428. [PubMed: 9931141]
92. Feng MG, Dukacz SA, Kline RL. Selective effect of tempol on renal medullary hemodynamics in spontaneously hypertensive rats. Am J Physiol Regul Integr Comp Physiol 2001;281(5):R1420–R1425. [PubMed: 11641111]
93. Fenoy FJ, Ferrer P, Carbonell L, et al. Role of nitric oxide on papillary blood flow and pressure natriuresis. Hypertension 1995;25(3):408–414. [PubMed: 7875767]
94. Ojo AO, Wolfe RA, Held PJ, et al. Delayed graft function: risk factors and implications for renal allograft survival. Transplantation 1997;63(7):968–974. [PubMed: 9112349]
95. Breza J, Navratil P. Renal transplantation in adults. BJU Int 1999;84(2):216–223. [PubMed: 10444155]
96. Gainza FJ, Minguela I, Lopez-Vidaur I, et al. Evaluation of complications due to percutaneous renal biopsy in allografts and native kidneys with color-coded Doppler sonography. Clin Nephrol 1995;43(5):303–308. [PubMed: 7634544]
97. Preda A, Van Dijk LC, Van Oostaijen JA, et al. Complication rate and diagnostic yield of 515 consecutive ultrasound-guided biopsies of renal allografts and native kidneys using a 14-gauge Biopty gun. Eur Radiol 2003;13(3):527–530. [PubMed: 12594555]
98. Sadowski EA, Fain SB, Alford SK, et al. Assessment of acute renal transplant rejection with blood oxygen level-dependent MR imaging: initial experience. Radiology 2005;236(3):911–919. [PubMed: 16118170]
99. Djamali A, Sadowski EA, Samaniego-Picota M, et al. Noninvasive assessment of early kidney allograft dysfunction by blood oxygen level-dependent magnetic resonance imaging. Transplantation 2006;82(5):621–628. [PubMed: 16969284]
100. Colvin RB. Chronic allograft nephropathy. N Engl J Med 2003;349(24):2288–2290. [PubMed: 14668453]
101. Wu G, Luo F, Li Z, et al. Transient relationships among BOLD, CBV, and CBF changes in rat brain as detected by functional MRI. Magn Reson Med 2002;48(6):987–993. [PubMed: 12465108]
102. Zhao JM, Clingman CS, Narvainen MJ, et al. Oxygenation and hematocrit dependence of transverse relaxation rates of blood at 3T. Magn Reson Med 2007;58(3):592–597. [PubMed: 17763354]
103. Spees WM, Yablonskiy DA, Oswood MC, et al. Water proton MR properties of human blood at 1.5 Tesla: magnetic susceptibility, T(1), T(2), T*(2), and non-Lorentzian signal behavior. Magn Reson Med 2001;45(4):533–542. [PubMed: 11283978]
104. Hess W. Affinity of oxygen for hemoglobin--its significance under physiological and pathological conditions. Anaesthesist 1987;36(9):455–467. [PubMed: 3318547]
105. Grenier N, Basseau F, Ries M, et al. Functional MRI of the kidney. Abdom Imaging 2003;28(2):164–175. [PubMed: 12592462]
106. Wang ZJ, Yeh BM. Is assessing renal oxygenation by using blood oxygen level-dependent MR imaging a clinical reality? Radiology 2008;247(3):595–596. [PubMed: 18487526]

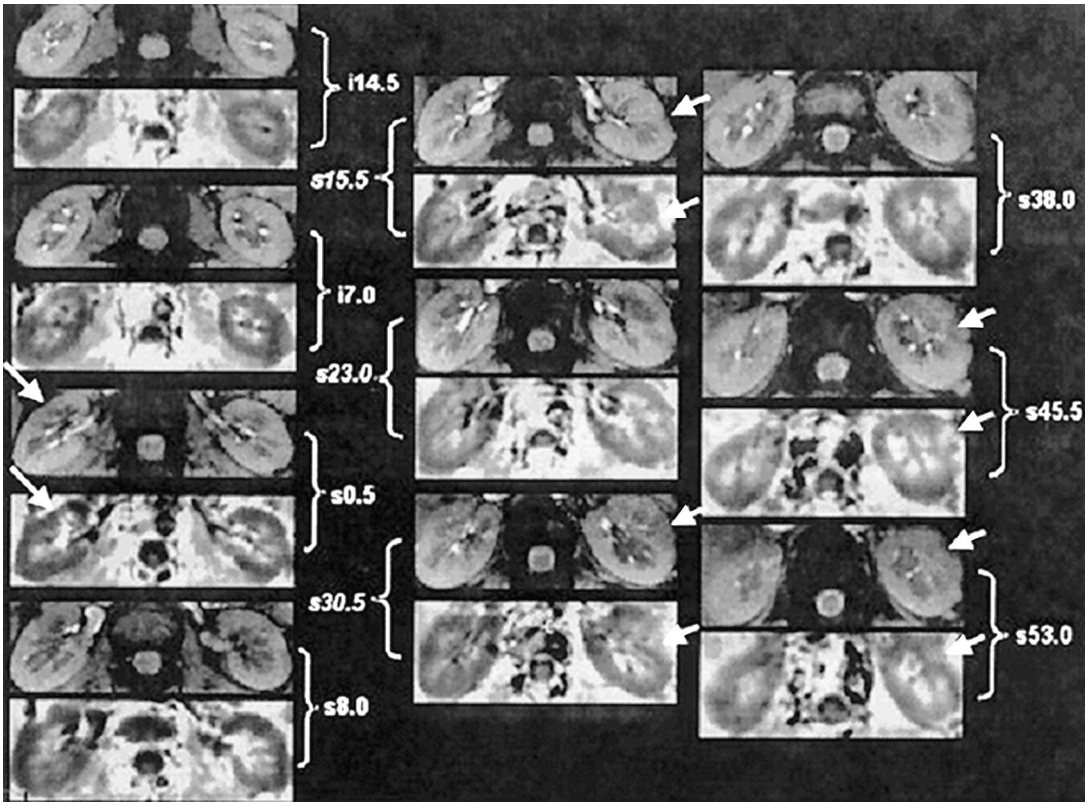

Figure 1.

Images obtained with the mGRE sequence in one representative healthy subject. Ten pairs of baseline anatomic (top) and R_2* (bottom) images from different slices covering the entire kidney. The anatomic image is usually the first image of the series of 16 GRE images. The R_2* map was obtained by fitting the signal intensity *vs.* TE data to a single decaying exponential function. Note that in the R_2* map, the medulla appears brighter than the cortex, implying a higher R_2* value in the medulla, which in turn implies higher deoxyhemoglobin content or less tissue oxygenation. The arrows point to obvious bulk susceptibility-induced artifacts, probably due to the presence of bowel gas in close proximity. The MRI parameters used in this scan were: TR/TE/flip angle/BW/FOV=65/7~40.1ms/30/62.5kHz/36cm at 3.0T with matrix size 256×256 and 0.75 phase FOV. (From Li LP, Vu AT, Li BS, Dunkle E, Prasad PV. Evaluation of intrarenal oxygenation by BOLD MRI at 3.0 T. J Magn Reson Imaging. 2004 Nov;20(5):901-4; with permission)

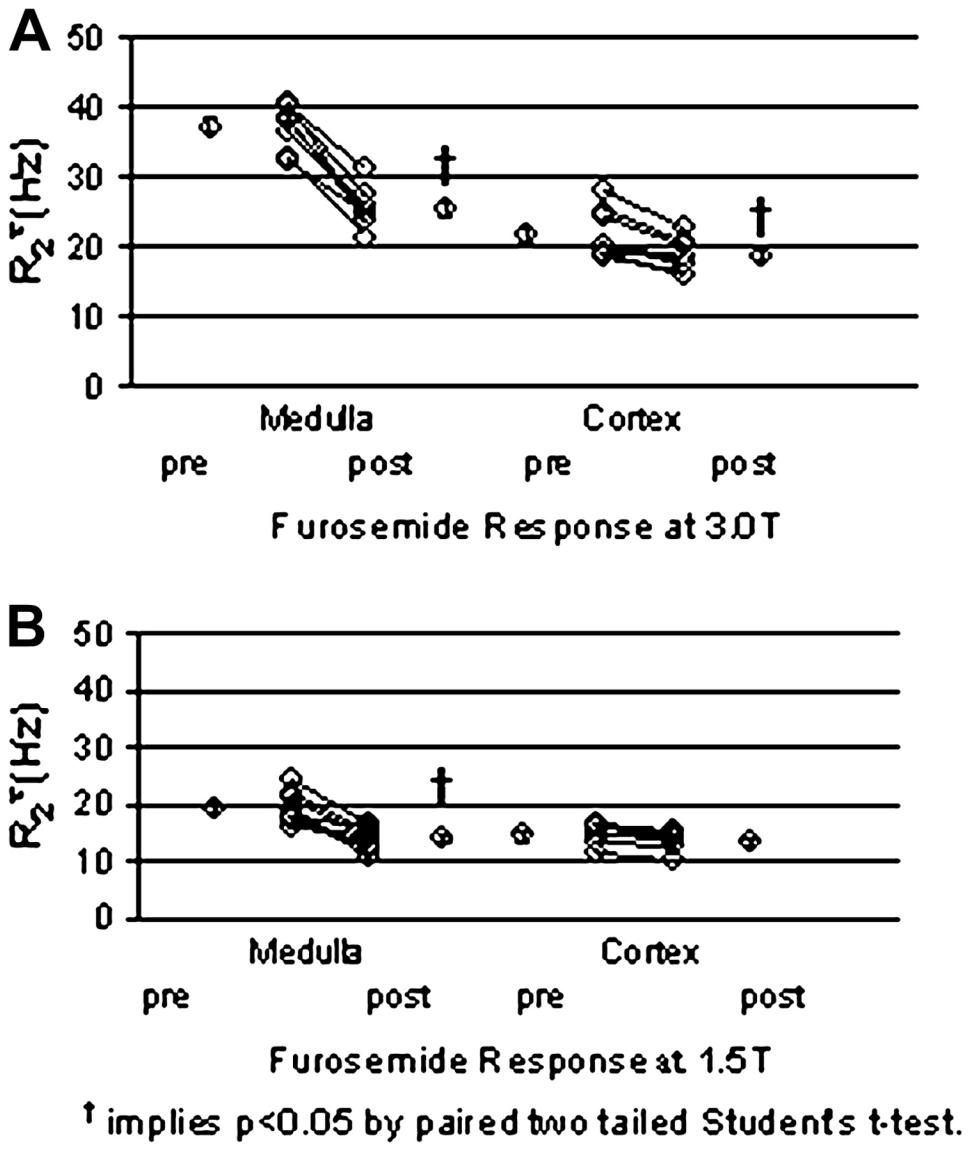

Figure 2.

(a) Summary of individual changes in medullary and cortical R_2* post furosemide in healthy young volunteers at 3.0T. (b) Similar data obtained at 1.5 T in a different group of healthy young subjects. (From Li LP, Vu AT, Li BS, Dunkle E, Prasad PV. Evaluation of intrarenal oxygenation by BOLD MRI at 3.0 T. J Magn Reson Imaging. 2004 Nov;20(5):901-4; with permission)

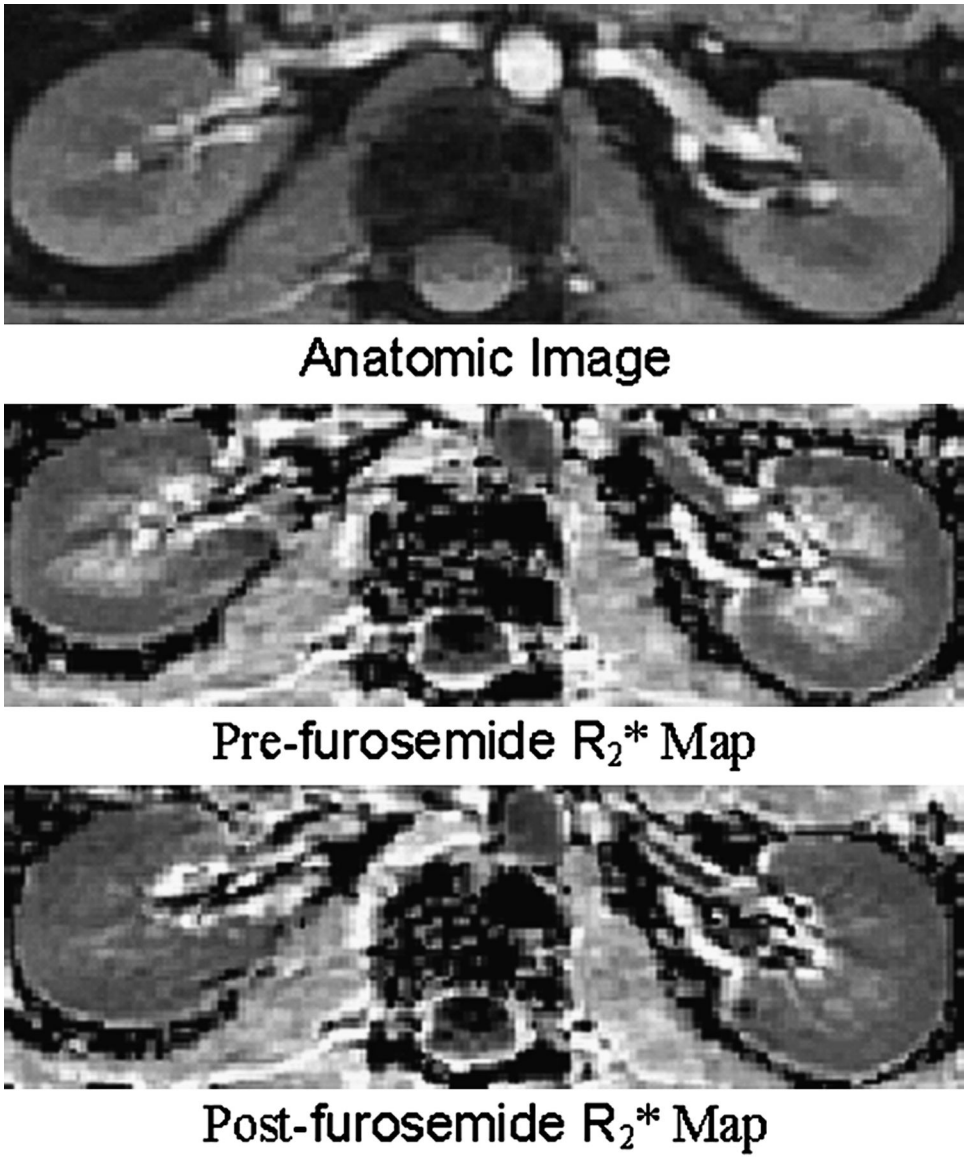

Figure 3.

Representative images obtained with the mGRE sequence in a healthy subject pre- and post-furosemide administration. Top is the anatomic image of the kidney (first image of the series of 16 GRE images). Middle is the pre-furosemide R_2* map, and at the bottom is the post-furosemide R_2* map obtained at the same slice location. The windowing was held constant for both the maps. Note that the medulla appears much brighter than the cortex on the pre-furosemide R_2* map, but looks close to isointense compared to the cortex on the post-furosemide R_2* map, implying improved oxygenation on the latter. (From Li LP, Vu AT, Li BS, Dunkle E, Prasad PV. Evaluation of intrarenal oxygenation by BOLD MRI at 3.0 T. J Magn Reson Imaging. 2004 Nov;20(5):901-4; with permission)

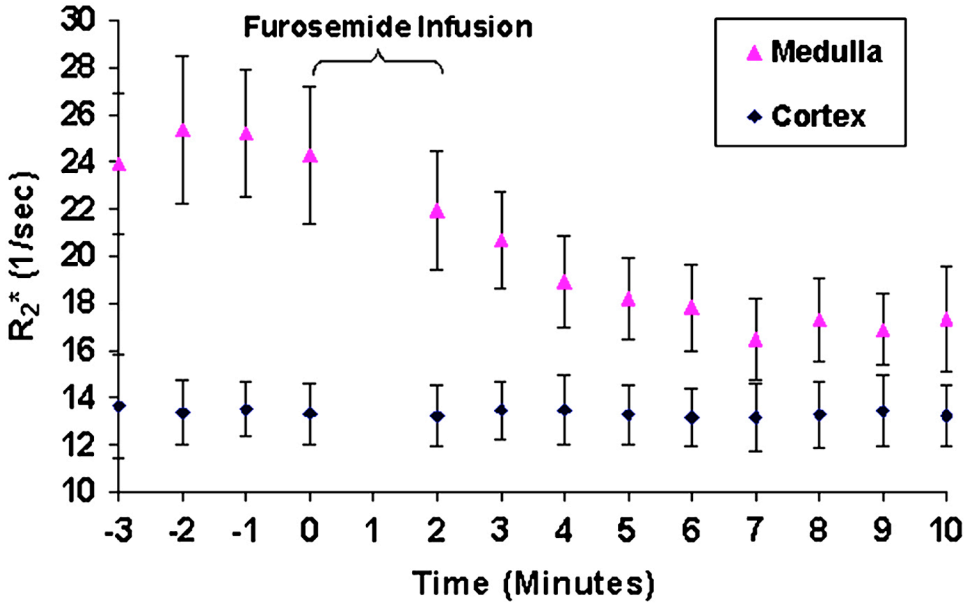

Figure 4.

A graphical representation of the R_2^* values as a function of time obtained in one representative subject. The first 4 points represent the mean baseline R_2^* values. Zero on the time axis represents the time of furosemide administration. The error bars represent the standard deviation of the pixel data for all of the regions of interest used to determine a single time point. Note that the cortical R_2^* remain relatively constant over the entire acquisition period, whereas medullary R_2^* approaches that of the cortex after administration of furosemide. (From Tumkur S, Vu A, Li L, Prasad PV. Evaluation of intrarenal oxygenation at 3.0 T using 3-dimensional multiple gradient-recalled echo sequence. Invest Radiol. 2006 Feb;41(2):181-4; with permission.)

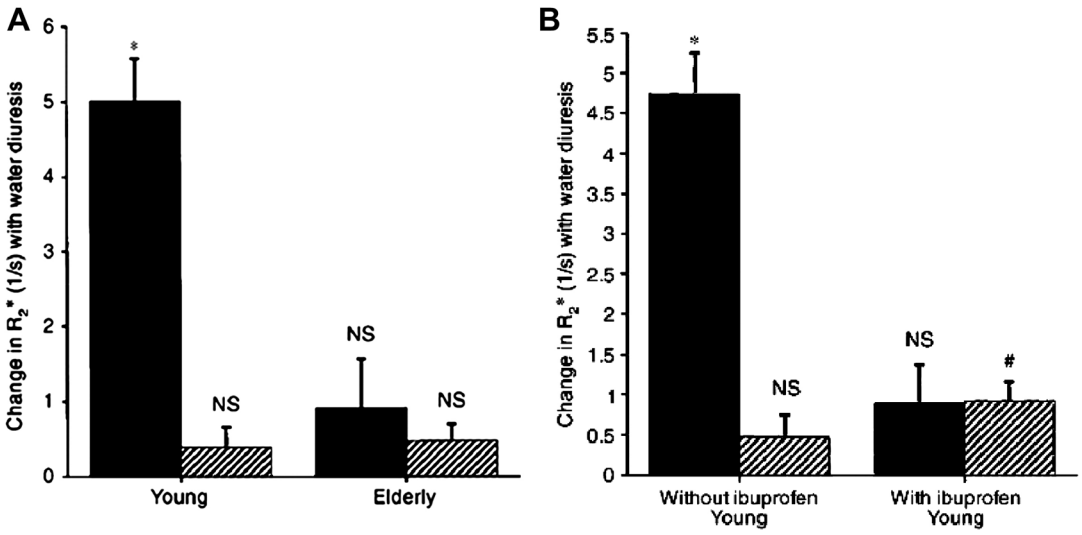

Figure 5.

(A): Comparison of changes in R_2* in response to water load in 9 young and 9 elderly subjects. (B): Comparison of changes in R_2* in response to water load in 6 young subjects with and without cyclooxygenase inhibition with ibuprofen. Symbols are: (■) medulla; (▨) cortex. Columns are mean ± SEM. NS implies not significant, * implies $p<0.01$, and # implies $p<0.02$.. (From Prasad PV, Epstein FH. Changes in renal medullary pO_2 during water diuresis as evaluated by blood oxygenation level-dependent magnetic resonance imaging: effects of aging and cyclooxygenase inhibition. Kidney Int. 1999 Jan; 55(1):294-8; with permission.)

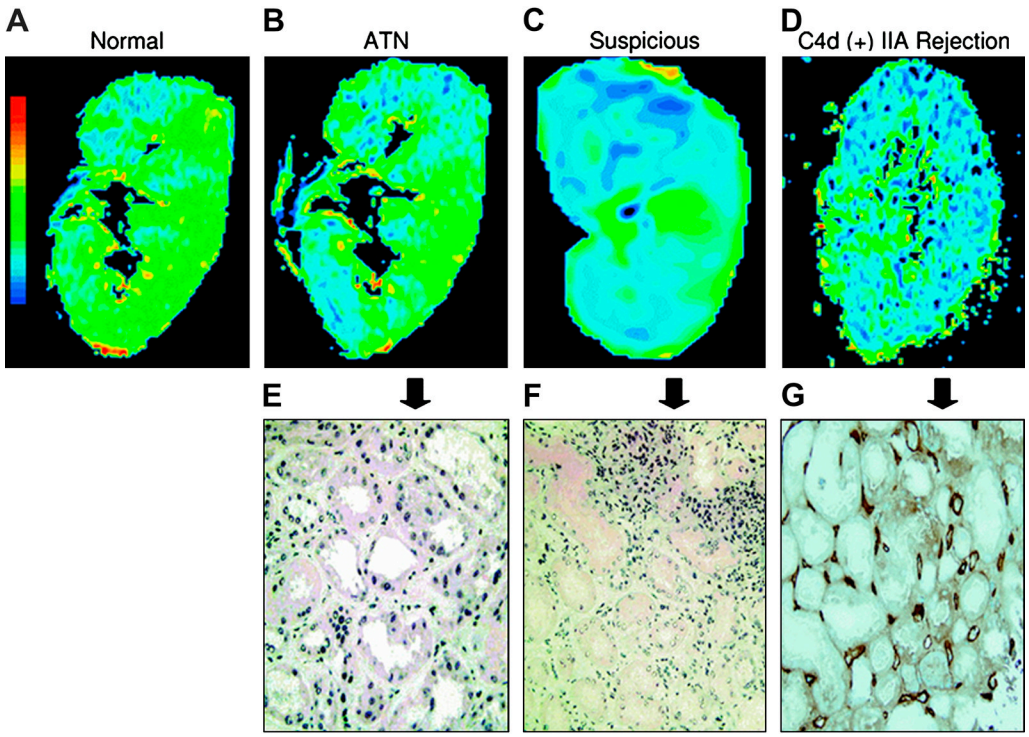

Figure 6.

BOLD-MR color R_2* map of coronal sections and corresponding histopathological findings. (a–d) Color R_2* maps in the coronal planes, of normal kidney allograft and transplants with acute dysfunction. Blue represents the lowest R_2* value (lowest deoxyhemoglobin concentration), and green, yellow, and red show increasing R_2* values. Color map scale is similar in all figures. (e–g) Pathology sections (20 × magnification) of the corresponding kidney with ATN (e), suspicious for rejection (f) and C4d (+) IIA rejection (g with insert). (From Djamali A, Sadowski EA, Samaniego-Picota M, Fain SB, Muehrer RJ, Alford SK, Grist TM, Becker BN. Noninvasive assessment of early kidney allograft dysfunction by blood oxygen level-dependent magnetic resonance imaging. Transplantation. 2006 Sep 15;82(5):621-8; with permission.)